Maternal obesity programs cardiac remodeling in offspring via epigenetic, metabolic, and immune dysregulations

Authors: Elysse A. Philips[1], Yem Alharithi[1], Tim D. Wilson[1], Cameron Broberg[1], Brett A. Davis[1], Sheryl Koch[3], Lucia Carbone[1,2,4], Jack Rubinstein[3], Susan B. Gurley[5], Sandra Rugonyi[1,6], Sushil Kumar[7], and Alina Maloyan[1].

Affiliations:

[1]Department of Medicine, Knight Cardiovascular Institute, Oregon Health & Science University, Portland, OR, 97239

[2] Department of Molecular and Medical Genetics, Oregon Health & Science University, Portland, OR, 97239

[3]Division of Cardiovascular Health and Disease, Department of Internal Medicine, College of Medicine, University of Cincinnati, Cincinnati, OH, 45221

[4]Division of Genetics, Oregon National Primate Research Center, Beaverton, OR, 97315

[5]Department of Medicine, University of Southern California, Los Angeles, CA

[6]Department of Biomedical Engineering, Oregon Health & Science University, Portland, OR, 97239

[7]Department of Cell, Development and Cancer Biology, Knight Cancer Institute, Oregon Health & Science University, Portland, OR, 97239

Corresponding Author: Alina Maloyan, PhD, FAHA. Knight Cardiovascular Institute, Oregon Health and Science University, 3181 SW Sam Jackson Park Rd, Portland, Oregon, 97239. Email: maloyan@ohsu.edu; phone: 503-494-0012.

Running Title: Cardiac dysfunction in the offspring of obese mothers.

Keywords: maternal obesity, developmental programming**,** cardiac epigenetics, inflammation.

Declaration of Interests: none

Grant Support and Acknowledgements. We thank Kim Montaniel for his help with measurements of mean arterial pressure. Financial support for this work was provided by the NIH HL170097, HL164474, HD099367, HD118370, OHSU Exploratory Research Seed Grants, and OHSU Medical Research Foundation (to A.M.). The University of Cincinnati Mouse Metabolic Phenotyping Center was funded by the NIDDK (National MMPC, RRID:SCR_008997, www.mmpc.org) under the MICROMouse Program, Grants DK076169. We acknowledge the KCVI Epigenetics Consortium, the Massive Parallel Sequencing Shared Resource, and the Advanced Computing Center at OHSU.

Author Contributions: SK, SR and AM conceived and designed the study ; EAP, YA, TDW, and CB conducted the experiments; SBG provided guidance and access to the tail cuff blood pressure measuring system, ShK and JR analyzed echocardiography data; SK planned flow cytometry experiments and helped with data analysis; BD and LC performed DNA methylation profiling and analyzed the data; SR and AM acquired funding; AM wrote the manuscript. All authors provided feedback and assisted with preparing the final manuscript.

Data Availability. DNA methylation data were submitted to Gene Expression Omnibus (GEO) repository, the accession number is GSE294642.

Abstract

Maternal obesity during pregnancy significantly increases the offspring's risk of later-life cardiovascular disease. This study investigated cardiometabolic perturbations by utilizing a mouse model of maternal high-fat diet (HFD)-induced obesity that recapitulates metabolic abnormalities observed in humans. We report that offspring of HFD-fed mothers (Off-HFD) exhibit a progression of obesity, hypertension, dyslipidemia, and metabolic inflexibility when compared with offspring of regular diet-fed mothers (Off-RD). Deeper investigation of cardiac function further identified significant functional, metabolic, and immune perturbations in adult offspring of mothers on HFD. Specifically, Off-HFD mice presented progressing cardiac hypertrophy with reduced ejection fraction, increased accumulation of fibrotic tissue, mitochondrial dysfunction, and altered immune complexity including increases in cardiac resident and infiltrated macrophages, and decreases in CD4+ and CD8+ T-cell subpopulations. While these alterations may not be immediately catastrophic, they likely predispose the offspring to heightened sensitivity to nutritional, psychological, or environmental stressors. Analysis of DNA methylation in the hearts of newly-weaned offspring from RD and HFD mothers revealed numerous differentially methylated CpGs and regions within genes associated with cardiac development, hypertrophy, mitochondrial function, and immune response. Thus, our study shows epigenetic remodeling early in development, which is likely responsible for the cardiovascular dysregulation observed in adult life. These findings uncover potential windows of opportunity for preventive therapy and early therapeutic interventions.

INTRODUCTION

Obesity is a rapidly growing health concern; in the last 30 years, its presence in the United States has doubled(1). In 2022, the worldwide prevalence of obesity among adults was 16% (890 million), with 43% (2.5 billion) being overweight (2). Similarly, the prevalence of overweight and obesity among women of reproductive age (15-49 years old) has increased from 28.4% in 1999-2000 to 41.5% in 2016 (3) and is becoming a serious public health issue. Importantly, obesity promotes cardiovascular disease via dysregulations in endothelial function and vascular remodeling that cause atherosclerotic and vasospastic coronary heart disease, arrhythmias, cardiomyopathy, and congestive heart failure (2, 4). In the pregnancy context, both pre-gestational obesity and greater than healthy gestational weight gain complicate pregnancy *per se* and significantly increase the risk of adverse outcomes (2). Moreover, obesity in pregnancy programs the offspring to become obese and to develop later-life cardiovascular and metabolic diseases, including Type II diabetes (5-9). Thus, maternal obesity is a key element in a positive-feedback loop, initiating a vicious intergenerational cycle of obesity that cannot be explained by genetics or lifestyle choices (10, 11).

A typical pregnancy depends on the tightly-regulated transfer of nutrition to the fetus, which is governed through extensive fetal-maternal communication. Consequently, alterations in maternal health and perturbation of that communication leave long-lasting imprints on the fetus, an effect known as developmental programming, that can result in structural and physiological abnormalities that present as disease later in the offspring's life. Epidemiological data link obesity in pregnancy with major birth defects, including neural tube and cardiac defects (12), and with increased risk of neurodevelopmental disorders, including cerebral palsy, attention-deficit disorder, cognitive delay, and even autism (13-15). Likewise, there is a clear epidemiologic correlation between increased maternal BMI and offspring cardiovascular disease (2, 16). A systematic review of five studies assessing the relationship between maternal obesity and congenital heart diseases found a significant correlation (17), and another review of 14 studies found a dose-response effect between maternal weight and offspring heart disease (18). More broadly, children born to obese mothers present structural and functional cardiovascular dysregulations that increase the likelihood of later-life cardiac events and premature mortality (5, 19-28). Thus, early-life adversity stemming from maternal obesity establishes a susceptibility to cardiovascular disease throughout life.

Building on our established mouse model of maternal high-fat diet (HFD)-induced adiposity, which replicates metabolic abnormalities seen in offspring of obese mothers (including obesity, glucose intolerance, and asthma (29-31)), this study tested the hypothesis that maternal HFD independently drives offspring cardiovascular dysfunction, separate from the influence of adverse postnatal lifestyle factors. We further examined the effects of maternal HFD on offspring cardiac function, epigenetics, metabolism, and immune complexity.

MATERIALS AND METHODS

Study approval. All animal experiments were approved by Oregon Health & Science University's Institutional Animal Use Committee (IACUC protocol # IP00432).

Antibodies. Total OXPHOS Rodent Western Blot Antibody Cocktail was purchased from Abcam (Waltham, MA, cat # ab110413). Antibodies against Vinculin, p62 and Rubicon were purchased from Cell Signaling (Danvers, MA, cat # 4650, 5114 and 8465 respectively). Anti-DGAT1 antibody was purchased from Proteintech (Rosemont, IL, cat # 11561-1-AP), and the antibody against autophagy regulator TFEB was purchased from Invitrogen (Waltham, MA, cat #PA1-31552).

Mouse model of maternal obesity. All mouse studies were done using wild-type FVB/N mice. Mice were kept under a 12-hour light/dark cycle in temperatures between 18-23 degrees Celsius with 40-60% humidity, in stress-free/bacteria-free conditions. Mice were caged in groups of three to five whenever possible. Food and water were given ad libitum, and body weight was determined weekly. To induce maternal obesity, a high-fat diet (Teklad Cat#TD.06415) or its control, a regular diet (RD, PicoLab® Laboratory Rodent Diet Cat # 5L0D), was given to virgin female FVB/NJ mice from six weeks of age and throughout the entire study. The diet compositions have been reported before (32) After eight weeks of dietary intervention, RD- and HFD-fed female mice were bred to an age-matched RD-fed male. Offspring were fed the RD only starting from weaning and throughout their life.

Metabolic phenotyping. Oxygen consumption and respiratory exchange ratio (RER) were measured in individually housed mice by Vanderbilt University's Mouse Metabolic Phenotyping Core using the Promethion from Sable Systems (Las Vegas, NV).

Mean arterial pressure was non-invasively measured using a CODA® tail-cuff blood pressure system (Kent Scientific, Torrington, CT) after two weeks of training.

Blood lipid profiling was performed at the Mouse Metabolic Phenotyping Center of the University of Cincinnati. Plasma triglycerides were measured using the Randox Triglyceride Assay Kit (Randox Laboratories, Kearneysville, WV). Plasma cholesterol levels were determined using the Infinity Total Cholesterol Assay Kit (Fisher Scientific, Waltham, MA). Plasma phospholipids were assessed using the Phospholipids C Assay (Wako Life Sciences, Inc., Mountain View, CA). Plasma non-esterified fatty acids were measured using the Wako HR Series NEFA-HR (2) (Wako Life Sciences, Inc., Mountain View, CA). All measurements were conducted according to the manufacturer's instructions.

Transmission electron microscopy. Hearts were perfused with 3.5% glutaraldehyde in 0.1 M/L phosphate buffer, pH 7.4 and embedded in Embed 812 resin (Electron Microscopy Science) for sectioning. The ultrathin sections were visualized by the Multiscale Microscopy Core at OHSU using a FEI Tecnai™ with iCORR™ transmission electron microscope (Thermo Fisher Scientific, Hillsboro, Oregon).

Protein isolation. Proteins were isolated from mouse hearts and lysed using ice-cold radioimmunoprecipitation assay buffer with freshly-added protease and phosphatase inhibitors. The resulting mixture was transferred to a 1.5 ml tube and centrifuged at 1000 x *g* for ten minutes at 4 °C to remove cellular debris. The supernatant was then transferred to a fresh tube and protein concentration quantified using a Pierce Bicinchoninic Acid Protein Assay Kit (Thermo Fisher Scientific, Waltham, MA).

Western blotting. Myocardial proteins (10-25 mg) were separated on a 4-20% SDS-PAGE gel, then transferred to a polyvinylidene difluoride membrane and blocked for one hour in 5% (w/v) milk in TBS solution with 0.1% Tween 20. Membranes were subsequently incubated overnight with primary antibodies, washed, blocked in 1% milk, and probed with secondary antibodies conjugated to HRP. Western blot membranes were visualized using G:Box and analyzed using

GeneTools, both utilities from Syngene (Frederick, MD). All samples were normalized to housekeeping genes.

RRBS method and analysis. DNA methylation was evaluated using reduced representation bisulfite sequencing (RRBS) (33), a genome-wide approach that allows the capture of key regulatory regions including promoters, CpG islands, and CpG island shores. RRBS libraries were generated by the Knight Cardiovascular Institute Epigenetics core using established methods (34, 35). Briefly, genomic DNA from left ventricle samples were digested overnight with *Msp*I (New England Biolabs) to produce sticky ends starting with a CpG. Libraries were then prepared using the NEXTflex Bisulfite-Seq Kit (BioScientific) and bisulfite conversion was performed with the EZ DNA Methylation-Gold Kit (Zymo Research). After quality control, libraries were multiplexed and sequenced on a NovaSeq 6000 at the OHSU Massively Parallel Sequencing Shared Resource to obtain roughly 40 million reads/library. Sequencing data were downloaded and analyzed as described in Carbone et al. (34). Briefly, after evaluation with FastQC (Andrews, 2010. http://www.bioinformatics.babraham.ac.uk/projects/fastqc), read alignment to the mouse reference genome (mm10) and methylation calling on every covered cytosine were performed with Bismark (36). Coverage files from Bismark methylation extractor were used to obtain the coverage and methylation rate of each covered CpG. A methylation rate table was constructed to include only CpGs with minimum 10X coverage and found on canonical chromosomes (1-19 and X,Y). For differential analysis, the table was subset to include CpGs with at least 10X coverage in at least 2 replicates per group of maternal diet (High Fat Diet or Regular Diet) resulting in 421,177 CpGs. Limma (37) was used for differentially methylated cytosine (DMC) analysis. To stabilize variance and improve normality, methylation percentages were transformed using the **arcsin square root transformation**. A linear model was fitted with sample groups and sex as covariates, and empirical Bayes moderation was applied to estimate DMCs. Statistical significance was determined using **moderated t-tests**, and multiple testing correction was performed using the **Benjamini-Hochberg false discovery rate (FDR)** method. Comb-p (38) was used for differentially methylated region (DMR) analysis, using the p-values obtained from DMC analysis as input. The following parameters were used with comb-p pipeline: -c 4 --dist 300 --seed 0.05 --step 60. Genes overlapping or close to DMRs were annotated using custom scripts, and pathway enrichment analyses were conducted using publicly available tools (e.g. GREAT, *EnrichR*) (39, 40). To examine potential transcription factors involved in the dysregulation of key genes/pathways, we used Hypergeometric

Optimization of Motif EnRichment (HOMER) (41) to detect enriched binding motifs in the putatively functional DMRs.

To visualize sample similarity in terms of methylation profiles, we performed principal component analysis on the methylation percentages of 343,296 CpGs with at least 10X coverage; the resulting plot is presented in **Supplemental Figure 1**. One male Off-HFD sample was excluded due to low coverage. A few samples appeared to segregate away from the cluster formed by the rest; these few also showed the highest methylation in non-CpG contexts. When those segregated samples were excluded, the plot showed female Off-RD to cluster with female Off-HFD, and males to similarly cluster together (**Supplemental Figure 1**).

Gene Ontology and pathway analysis. Enrichment analysis of Gene Ontology (release date 20210101) terms was performed for genes associated with differentially methylated CpGs (DMCs) and DMRs using Panther (release date 20200728). Hypo- and hypermethylated regions were jointly analyzed for overrepresentation using Fischer's exact test with FDR correction (FDR<0.05), with fold enrichment of over- and underrepresented pathways reported relative to the whole mouse genome (which was used as the reference list) (33). Pathway analysis of DMR genes was conducted using Ingenuity Pathway Analysis (Qiagen, Redwood City, CA) and STRING (Version 12.0).

Transcription factor binding site analysis. Enrichment of transcription factor binding sites within DMRs was performed using HOMER (41).

Echocardiography. Mice were anaesthetized with isoflurane and subjected to echocardiography at the Small Animal Research Imaging Center at OHSU using Vevo LAB 3.1.1 (FUJIFILM VisualSonics, Inc.). Cardiac function and structure values were obtained from B mode images from the parasternal long axis (PSLAX). Left ventricular diameter (LVID), posterior wall (LVPW) and intraventricular septum (IVS) were measured in both systole (s) and diastole (d). B-mode PSLAX were used to calculate ejection fraction (EF), LV mass and stroke volume (SV). Stroke volume was calculated as the product of the left ventricular (LV) outflow tract cross-sectional area and velocity-time integral on angle-corrected pulsed-wave Doppler. LV end-diastolic and end-systolic volumes were calculated from short-axis linear dimensions and long-axis dimensions using established geometric assumptions.

Western blotting. Myocardial proteins (10-25 mg) were separated on a 4-20% SDS-PAGE gel, then transferred to a polyvinylidene difluoride membrane and blocked for one hour in 5% (w/v) milk in TBS solution with 0.1% Tween 20. Membranes were subsequently incubated overnight with primary antibodies, washed, blocked in 1% milk, and probed with secondary antibodies conjugated to HRP. Western blot membranes were visualized using G:Box and analyzed using GeneTools, both utilities from Syngene (Frederick, MD). All samples were normalized to housekeeping genes.

Histology. H&E and Masson trichrome staining were performed at the OHSU Histopathology Core. Trichrome-stained sections were used to evaluate myocyte cross-sectional area with the aid of ImageJ (National Institutes of Health, Bethesda, Maryland).

Flow cytometry. The list of antibodies is presented in **Supplemental Table 1**. In preparation for flow cytometry, nearly 10^6 cells from individual hearts were first incubated on ice for 30 min in a solution consisting of 1:10 Fc Receptor Binding Inhibitor (eBiosciences) and 1:500 Live/Dead Aqua stain (Invitrogen) in PBS. Cells were then combined with fluorescently-labeled monoclonal antibodies as previously described (42) in a solution of PBS + 5% FCS + 1.0 mM EDTA (FACS buffer). After another 30 min incubation on ice, the cells were washed 1x with FACS buffer. Next, the stained cells were treated with permeabilization/fixation buffer (eBioscience) on ice for ten minutes, then washed 1x using permeabilization buffer (eBioscience). The permeabilized cells were then subjected to intracellular staining by incubation with fluorescently-labeled monoclonal antibodies in FACS buffer for 30 minutes on ice. Finally, flow cytometry data was acquired on a Cytek Aurora (Cytek Biosciences) spectral flow cytometer and analyzed using FlowJo software v9.5 (Ashland, OR).

Statistical analysis. Means were compared using two-way analysis of variance (two-way ANOVA) followed by Student’s *t*-test (corrected for multiple comparisons) or its non-parametrical equivalent. The obtained *p*-values are indicated in each respective graph. Significance was set at an alpha of 0.05. When no sex-dependent differences were found, the results from males and females were pooled.

RESULTS

Physiological changes in the mouse offspring of obese mothers.

Six-week-old females were placed on either a regular (13% kcal from fat) or a high-fat (45% kcal from fat) diet (RD and HFD, respectively) (**Fig.1A**). After eight weeks of dietary intervention, the females were bred to RD-fed males. Birthweights were significantly lower in the offspring of HFD-fed mothers (Off-HFD) when compared with offspring of RD-fed mothers (Off-RD) (**Fig.1B**). However, despite being born smaller, both male (**Fig.1C**) and female Off-HFD (**Fig.1D**) caught up by weaning (3-week-old) and then remained heavier than Off-RD mice throughout their life.

Whole body metabolic alterations in the offspring of HFD-fed mothers.

Despite the fact that Off-HFD mice show consistent increase in body weight and percentage of fat (29), surprisingly, no between-group differences in food intake and activity levels were observed (32). We next assessed the effects of maternal obesity on whole-body metabolic parameters in adult 16-week-old Off-RD and Off-HFD mice. This assessment revealed no significant changes in the 24-hour pattern of oxygen consumption (**Fig.2A-B**). However, significant alterations were identified in respiratory exchange ratio (RER, **Fig.2C-D**). In Off-RD mice, the 24-hour oscillation in RER, an indicator of substrate utilization between active and resting periods, alternated between high values (utilization of carbohydrates) in active periods and low values (utilization of fats) during resting periods (**Fig.2C-E**). These oscillations were completely abolished in Off-HFD mice (**Fig.2C-D, F**), suggesting metabolic inflexibility, and daily RER was significantly lower in Off-HFD vs. Off-RD (**Fig.2G**).

Cardiovascular and metabolic perturbations in the offspring of HFD-fed mothers.

We next focused on the impact of maternal obesity on cardiovascular remodeling in offspring. At three weeks of age, newly weaned Off-HFD mice showed a moderate (8.6%) increase in heart-weight-to-body-weight ratio as compared with age-matched Off-RD mice (p=0.0005, **Fig.3A**). By six months of age, Off-HFD mice showed more dramatic 60% increase in heart weight to body weight ratios, indicating a progressive hypertrophy phenotype (**Fig.3B**). No changes were observed in liver weight-to-body weight ratio in these mice (**Fig.3C**). We further measured mean arterial pressure in 16-week-old Off-RD and Off-HFD mice using a tail cuff sphygmomanometer, and found a significant increase in male Off-HFD mice but no change in female Off-HFD mice (**Fig.3D**). Blood lipid profiling revealed significantly increased levels of total cholesterol, triglycerides, phospholipids, and non-esterified fatty acids in both male and female Off-HFD vs. Off-RD, suggesting dyslipidemia (**Fig.3E-H**).

We then conducted cardiac function assessments in adult 24-30-week-old male and female Off-HFD and Off-RD mice using echocardiography. The majority of echocardiographic parameters were not significantly different between the groups (**Supplemental Table 2**); however, our data importantly revealed sexual dimorphism in offspring cardiac response to maternal obesity (**Figure 4A**). Specifically, IVS;d and LVPW;s were increased in male but not female Off-HFD vs. Off-RD (**Fig.4B, E**), probably due to increased mean arterial pressure (though IVS;s, and LVPW;d trended to be increased as well, neither reached statistical significance(**Fig.4C-D**)). In contrast, ejection fraction was reduced only in female Off-HFD vs. Off-RD mice (**Fig.4F**). Notably, the opposite sex-specific difference was observed among Off-RD mice, with male mice having significantly lower ejection fraction than females with these differences being abolished in Off-HFD mice (**Fig.4F**).

DNA methylation pattern in left ventricle is affected in newly weaned Off-HFD mice.

Published evidence suggests that prenatal and early postconceptional periods comprise the critical window during which DNA methylation patterns are established (43-46). In light of the observed impacts of maternal obesity on progression of adult cardiovascular disease in offspring, we took a step back to reveal cardiac epigenetic processes that precede cardiovascular dysfunction in Off-HFD mice. To determine regions and individual CpGs with significant differential methylation between offspring of HFD- and RD-fed mothers, we conducted reduced representation bisulfite sequencing (RRBS) on left ventricular samples from newly weaned three-week-old male and female Off-RD and Off-FD. The number of reads obtained per sample before and after trimming is provided in **Supplemental Table 3.** To visualize sample similarity in terms of methylation profiles, we performed principal component analysis on the methylation percentages of 343,296 CpGs with at least 10 X coverage; the resulting plot is presented in **Supplemental Figure 1**. One male Off-HFD sample was excluded due to low coverage. Three samples appeared to segregate away from the cluster formed by the rest; these few also showed the highest methylation in non-CpG contexts. When those segregated samples were excluded, the plot showed female Off-RD to cluster with female Off-HFD, and males to similarly cluster together (**Supplemental Figure 1**).

Our analysis identified 89 significant DMCs present in both male and female Off-HFD vs. Off-RD (FDR<0.05, *p*-value<0.001, amplitude of change >10%). From those, we identified 32 CpGs that overlapped with annotated genes (**Fig.5A**). Importantly, our data show that only 22%

of the DMCs exhibited increased CpG methylation in Off-HFD mice. The single greatest reduction in CpG methylation (47%) was observed for the gene *Impact*, a transcriptional regulator associated with protein sequestering activity under the stress conditions such as amino acid starvation (47). Meanwhile, two genes tied for the greatest increase in CpG methylation (>20%): Ectonucleotide Pyrophosphatase/Phosphodiesterase 3 (*Enpp3*), an extracellular enzyme that acts as a mediator of cell-cell innate immune communication (48); and Centrosomal Protein 72 (*Cep72*), a component of centriolar satellites previously implicated in mitotic spindle formation (49).

To understand what biological networks in the heart are affected by differential methylation downstream of maternal HFD, we applied the Ingenuity Pathway Analysis software to all genes with DMCs (FDR<0.05, $p<0.05$, absolute differential methylation >10%), genes by direction of change (hyper- and hypo-methylated), and data from both sexes (**Fig.5B**). We found several networks to be affected by maternal obesity ($p< 0.05$), including Cell Signaling and Interaction, Inflammatory Response, Cell Cycle, Cancer, Cardiovascular System Development, and Immunological Disease.

In the analysis of DMRs, absolute methylation differences >10% were considered significant at a Šídák multiple comparison p-value <0.05. Overall, 61 DMRs were identified within protein-encoding genes (**Fig.5C**), with 13 hypermethylated and 48 hypomethylated. The top ten hyper- and hypomethylated DMRs and associated genes are given in **Supplemental Tables 4 and 5**. We utilized STRING network analysis to determine which protein interaction networks were most subject to methylation changes in Off-HFD mice. **Supplemental Table 6** presents the list of differentially methylated genes specifically involved in cardiovascular development and

function. Among the genes with differentially methylated DNA, we observed a significant enrichment of those involved in cardiac morphogenesis and development (*Adamts1, Eng, F2r, Jmjd6, Notch1, Nrap,* and *Nrp2*), cardiac hypertrophy (*Adgrf5, F2r, Twf1*), immune responses including macrophage differentiation and activation (*Adgrf5, Atp6v1g1, Cebpa, Epas1, F2r, Nfkbil1, Notch1, Pecam1,* and *Shb*), mitochondrial function (*Cebpa, Cry1, Epas1*), and autophagy (*Lamtor3, Snx20, Stx12*).

We next applied Ingenuity Pathway Analysis to genes with DMRs to identify enrichments of cellular pathways. This yielded 16 master regulators (**Supplemental Table 7**), of which 11 were inhibited in Off-HFD hearts (z-score<-2.0, $p<0.05$), including the transcriptional regulators

Yin Yang 1 (*yy1*) and Mastermind Like Transcriptional Coactivator 1 (*maml1*); peptidases ADAM Metallopeptidase with Thrombospondin Type 1 Motif 5 (*adamts5*) and Plasminogen Activator, Tissue Type (*plat*); cell adhesion molecule Fat Atypical Cadherin 1 (*fat1*); and the Mitogen-activated Protein Kinase 4 (*mapk4*) family. Activated networks (z-score >2.0, *p*<0.05) included those involving cytokine colony-stimulating factor 1 (*csf1*), which regulates the production, differentiation, and function of macrophages; enzyme tumor necrosis factor (TNF)-alpha-induced protein 3 (*tnfaip3*); and the metalloproteinase inhibitor *timp3*.

We further sought to identify possible enrichment in motifs for transcription factors binding sites in correspondence of DMRs using the Hypergeometric Optimization of Motif EnRichment (HOMER) tool (41). This analysis yielded 14 transcription factor binding motifs specifically enriched in DMRs (**Supplemental Table 8**), including motifs recognized by GA Binding Protein Transcription Factor Subunit Alpha (GABPA), a factor involved in regulation of energy metabolism in the heart (50); ETS Proto-oncogene 1 (ETS1), which plays a crucial role in cardiac function (51); and ETS Variant Transcription Factor 2 (ETV2), a major regulator of cardiac and vascular development (52-54).

Histological and metabolic changes in the heart of adult Off-HFD mice.

We next subjected Off-RD and Off-HFD hearts to routine histological analysis using H&E and trichrome-stained paraffin sections derived from four-month-old animals. **Figure 6** illustrates some of the pertinent pathological differences between Off-RD and Off-HFD hearts. While Off-RD mice demonstrated normal tissue architecture, Off-HFD mice displayed perivascular inflammatory cell infiltrations potentially related to early ischemia (**Fig.6A**). We additionally sectioned paraffin-embedded Off-RD and Off-HFD hearts and applied trichrome staining to identify possible areas of fibrosis that contain collagen (**Fig.6B**). This revealed greater interstitial fibrosis in Off-HFD vs. Off-RD hearts (**Fig.6B**), specifically a four-fold increase in total area of fibrosis per mouse (*p*=0.0095, **Fig.6C**). Quantification of cardiomyocyte cross-sectional area in trichrome-stained sections further showed that despite the hypertrophy, Off-HFD hearts had slightly but significantly decreased cross-sectional area compared with Off-RD hearts (*p*=0.011, **Fig.6D**).

We further assessed the ultrastructure of Off-RD and Off-HFD hearts using transmission electron microscopy. Although this evaluation did not show any gross alterations in cardiomyocytes, we found that the overall architecture of mitochondrial arrangement in relation to sarcomeres was significantly altered in Off-HFD hearts. While typically, mitochondria are densely packed in a well-organized array between sarcomeres, their transverse boundaries closely aligned with the Z-line, Off-HFD heart tissue showed bundles of mitochondria lacking this regular arrangement (**Fig.7A**). In addition, Off-HFD hearts presented accumulation of autophagic structures, including autophagosomes and autolysosomes (labeled with white asterisks), and increased number of lipid droplets (yellow arrows). To establish a link between irregular mitochondrial appearance and perturbed function, we performed western blots for protein subunits from five electron transport chain complexes (**Fig. 7B-H**). The results revealed significant decreases in expression of complexes 3 and 5 (**Fig.7F and H**), while no changes were observed for complexes 1, 2, and 4. As the electron microscopy images suggested accumulation of autophagic vacuoles in Off-HFD hearts (**Fig.7A**), we next measured the protein expression of regulators of autophagy at early (Transcription Factor EB, TFEB), mid (sequestosome p62), and late (Rubicon) stages of progression; however, no between-group differences were observed (**Supplemental Figure 2**).

Immune profiles of adult Off-RD and Off-HFD hearts.

Inflammation has been recognized as a pathogenic feature of cardiac metabolic dysfunction and fibrosis (55-57). Accordingly, we conducted flow cytometry to examine immune cell populations in the hearts of four-month-old male and female Off-RD and Off-HFD mice. The gating strategy is illustrated in **Supplemental Figure 3**. Our data revealed a decrease in $CD45^+$ cells (**Fig.8A**) alongside significant increases in $CD11b^+F480^+$ macrophages and $CD11b^-$ $F480^+$ resident macrophages in Off-HFD vs. Off-RD hearts (**Fig.8B-C**). In addition, T-cells were decreased in Off-HFD hearts, including $CD3^+$, $CD4^+$, and $CD8^+$ cells (**Fig.8D-F**).

DISCUSSION

While pharmacological interventions for obesity are advancing, the difficulty in reversing and maintaining weight loss due to relapse underscores the importance of prevention. Lifestyle choices are recognized as key determinants in the development of obesity and its comorbidities; however, findings from this study and others (16) highlight that intrauterine exposure to a maternal obesogenic diet also contributes to increased cardiovascular disease risk. Consequently, effective prevention strategies must start before birth and continue throughout the lifespan.

There is a substantial body of epidemiological data linking maternal obesity to cardiovascular dysfunction in offspring (16). Studies in children born to obese mothers have reported structural and functional cardiac dysregulations (58) including diastolic dysfunction, hypertrophy, and hypertension (58-61). Across animal models, intrauterine exposure to maternal obesity has also been shown to lead to cardiac hypertrophy in adult offspring, with structural and functional cardiac perturbations (62-64). In the present study, we utilized our mouse model of maternal diet-induced obesity to characterize how maternal environment affects offspring cardiac function. We focused our experiments on epigenetic, functional, metabolic, and immune aspects of the heart from offspring weaning to adult age. Consistent with epidemiological findings, our data revealed that despite being fed a regular diet only and living a stress-free life, offspring of HFD-fed mothers present dyslipidemia, cardiac hypertrophy, hypertension and perturbations in cardiac function in adult age. Importantly, our functional data show sexual dimorphism in cardiac adaptation to maternal obesity, with males being hypertensive and showing greater septal and posterior wall thickness in some (but not all) measurements, while females presented with reduced ejection fraction without any changes in LV diameter or volume. Similar increases in intraventricular septum thickness were previously reported in 14-, 20-, and 32-week-old human fetuses carried by obese mothers (65).

Notably, despite progressing cardiac hypertrophy, the cross-sectional areas of cardiomyocytes were reduced in Off-HFD mice, a surprising discovery that contrasts with previous reports (66). Reduced cross-sectional area could be explained by either remodeling of mitochondrial dysfunction or changes in signal transduction pathways such as p53, which has been shown to cause cardiomyocyte elongation without altering area (67). The mechanisms underlying this reduction are yet unclear, and experiments are underway to investigate this important phenomenon.

Intrauterine exposure to maternal obesity also has a demonstrated association with development of cardiac fibrosis (68-70). Interestingly, several groups have reported presence of cardiac fibrosis in animals that were placed on a high-fat diet feeding post-weaning (64). Our team has have previously reported cardiac fibrosis in non-human primate fetuses born to obese mothers (71). Data from this study also suggest accumulation of fibrotic tissue, although to lesser degree, in the hearts of adult Off-HFD mice even in the absence of superimposed dietary challenges.

Overall, our findings indicate an age-dependent progression of cardiac pathology in offspring of obese mothers. Maternal obesity clearly has long-lasting effects on offspring cardiac metabolism and contractile function via currently undefined mechanisms. While multiple mechanisms can detect alterations in contractility, we propose that a key component of this pathology is related to changes in mitochondrial respiration. Specifically, we found changes in cardiac energy metabolism, including reduced expression of subunits of complexes III and V of the mitochondrial electron transport chain, complexes that are crucial for cardiac development and function (72, 73). In addition, electron microscopy revealed alterations in mitochondrial positioning within the heart tissue ultrastructure. Previously, changes in cardiac mitochondrial structure and alignment and in activity of mitochondrial complexes have both been documented in a mouse model of maternal high-fat–high-sucrose diet (62). Importantly, the same study also revealed a transgenerational inheritance (both male- and female-transmitted) of cardiac mitochondrial defects in the descendants of obese females (62). Our electron microscopy data did not show any structural changes in cardiac mitochondria, which can be explained by differences in maternal diet (high-fat diet vs. high-fat–high-sucrose diet).

Mitochondrial dysfunction plays a crucial role in the programming effects of maternal obesity, potentially indicating metabolic inflexibility stemming from exposure to a dyslipidemic and inflamed intrauterine environment. We have previously reported that human neonates born to obese mothers exhibit systemic dyslipidemia that puts them at high risk of developing cardiovascular and metabolic diseases in later life (74). Here, despite being weaned to a regular diet only, adult Off-HFD mice also show development of dyslipidemia that includes greater levels of cholesterol, triglycerides, phospholipids, and non-esterified fatty acids. Our lab and others have previously demonstrated mitochondrial dysfunction and metabolic inflexibility in placentae of obese women (75) and in the hearts of sheep (76) and rats (77) born to obese mothers. Metabolic flexibility is clinically evaluated using indirect calorimetry by measuring the respiratory exchange ratio (RER), which represents the volume of carbon dioxide produced relative to the volume of oxygen consumed. Our findings revealed significantly lower RER values in adult Off-HFD mice, coupled with an impaired ability to transition between carbohydrate and lipid fuel sources during activity and rest, indicative of metabolic inflexibility. Similarly, low RER has previously been reported in obese individuals (78) and in patients with type 2 diabetes (79).

In addition to cardiac and metabolic features, pre-gravid obesity has been shown to modulate offspring immunity (80). While clinical studies are naturally limited in their investigative scope, several have profiled cord blood, shown to be an excellent representation of the fetal immune system at birth (81), and found changes in immune cell frequency and phenotype in the context of maternal obesity (82-85). Our previous reports have further identified accumulation of inflammation in the placentae of obese women, suggesting that maternal obesity exposes the fetus to chronic inflammation during development (86, 87). In our mouse model of maternal diet-induced obesity, a prior multiomics analysis of bone marrow and its myeloid cells in newly weaned Off-HFD and Off-RD mice uncovered significant metabolic and immune changes in the offspring of HFD-fed mothers (29, 31). This indicates that immune and immunometabolic disruptions in the offspring of obese mothers occur early, before the manifestation of symptomatic metabolic disease. This study revealed significant alterations in immune cell populations in adult Off-HFD hearts. More specifically, although total immune cell numbers were reduced, there were increases in resident cardiac macrophages and infiltrated macrophages, immune cells crucial for adaptive cardiac remodeling (88).

Expansion of resident macrophages has been already reported in response to immune challenge, and was found to be associated with excessive production of collagen and accumulation of cardiac fibrosis (89). T lymphocytes also play important roles in cardiac homeostasis and response to injury (90). Subsets of CD4+ nonspecific effector T cells have demonstrated the capability to protect against post-inflammatory fibrosis in an experimental model of myocarditis (91), and it has been suggested that cardiac CD8+T-cells regulate the conversion of both cardiac-resident macrophages and infiltrated macrophages into cardioprotective macrophages, which are essential for myocardial adaptive responses. Here, we observed reductions in both CD4+ and CD8+ T-cell subsets; however, the roles of these changes in the observed cardiac dysfunction remains unclear. Further refinement of cardiac macrophage and T-cell subtypes, along with a more comprehensive understanding of their roles in the response to an adverse maternal environment, remains crucial. Our laboratory is currently pursuing this line of investigation.

The above findings indicate that offspring cardiac adaptation to maternal obesity is underscored by metabolic, immune, and functional changes, prompting questions of when and how the maternal environment affects fetal hearts. Alterations in epigenetic modifications are key in regulating the functioning and expression of genes related to cardiovascular disease through various mechanisms such as DNA methylation, histone modification, and noncoding RNA regulation (92). Importantly, epigenetic changes have previously been described in the setting of maternal obesity (93, 94). A clinical study that included 40 mother-infant dyads revealed strong association of maternal blood metabolites with fetal umbilical cord blood DNA methylation patterns (95), and exposure to maternal obesity during development is associated with changes in global DNA methylation of CpG sites and islands in the offspring's white adipose tissue, specifically in genes involved in adipogenesis (96, 97). These findings suggest that epigenetic modifications may provide a mechanism for programming of obesity and dyslipidemia in the offspring of obese mothers. We and others have previously reported dysregulations of fetal cardiac miRNAs in a non-human primate model of maternal obesity (71, 98). In this study, we profiled the methylation status of cardiac genes in the hearts of newly weaned three-week-old mice with the aim of identifying sets of cardiac genes that are differentially methylated early in life, prior to the appearance of obesity and metabolic perturbations. The results revealed significant changes in DNA methylation for Off-HFD mice, with enrichment of genes responsible for cardiac development, cardiac hypertrophy, metabolism, and immune responses and inflammation. Further experiments are needed to determine 1) what is the contribution of differentially methylated genes and pathways to the functional, immune, and metabolic dysregulations seen in the offspring of obese mothers; and 2) does the differential cardiac methylation pattern in young Off-HFD persist into adult life and into future generations?

Collectively, our data revealed metabolic, functional, and immune perturbations in the hearts of offspring of obese mothers. We also identified early-life cardiac epigenetic modifications that precede later-life cardiac abnormalities. While the various observed alterations may not be immediately catastrophic, they likely enhance the susceptibility of the offspring to secondary nutritional, psychological, or environmental insults, and increase the risk of future cardiovascular disease. Heart disease remains the leading cause of death in the U.S., and many of the contributing risk factors, including high blood pressure and obesity, continue to become more widespread at alarming rates (2). Undoubtedly, unhealthy dietary and lifestyle choices increase a person's risk of developing cardiovascular disease. However, the present work suggest that exposure to maternal obesity *per se* predisposes the offspring to heart disease independent of their lifestyle choices. Understanding the mechanisms that underlie this predisposition could facilitate the prevention of cardiac dysfunction in future offspring of mothers with obesity, for example through targeted manipulation of immune cells or of mitochondrial function to reduce fibrosis and improve heart energy metabolism and contractility, areas that represent promising fields of active study.

REFERENCES

1. National Health and Nutrition Examination Survey 2017–March 2020 Prepandemic Data Files Development of Files and Prevalence Estimates for Selected Health Outcomes, (2021).
2. Martin SS, Aday AW, Allen NB, Almarzooq ZI, Anderson CAM, Arora P, et al. 2025 Heart Disease and Stroke Statistics: A Report of US and Global Data From the American Heart Association. Circulation. 2025;151(8):e41-e660.
3. Wang Y, Beydoun MA, Min J, Xue H, Kaminsky LA, Cheskin LJ. Has the prevalence of overweight, obesity and central obesity levelled off in the United States? Trends, patterns, disparities, and future projections for the obesity epidemic. Int J Epidemiol. 2020;49(3):810-23.
4. Welsh A, Hammad M, Piña IL, Kulinski J. Obesity and cardiovascular health. Eur J Prev Cardiol. 2024;31(8):1026-35.
5. Stefan Johansson EV, Maria Altman, Anna-Karin Edstedt Bonamy, Fredrik Granath, Sven Cnattingius. Maternal overweight and obesity in early pregnancy and risk of infant mortality: a population based cohort study in Sweden. BMJ. 2014;349:g6572.

6. Anne-Maj Samuelsson PAM, Marco Argenton, Michael R. Christie, Josie M. McConnell, Eugene H.J. M. Jansen, Aldert H. Piersma, Susan E. Ozanne, Denise Fernandez Twinn, Claude Remacle, Anthea Rowlerson, Lucilla Poston, and Paul D. Taylor. Diet-Induced Obesity in Female Mice Leads to Offspring Hyperphagia, Adiposity, Hypertension, and Insulin Resistance. Hypertension. 2007;51:383-92.
7. Lahti-Pulkkinen M, Bhattacharya S, Wild SH, Lindsay RS, Räikkönen K, Norman JE, et al. Consequences of being overweight or obese during pregnancy on diabetes in the offspring: a record linkage study in Aberdeen, Scotland. Diabetologia. 2019;62(8):1412-9.
8. Desai M, Jellyman JK, Han G, Beall M, Lane RH, Ross MG. Maternal obesity and high-fat diet program offspring metabolic syndrome. Am J Obstet Gynecol. 2014;211(3):237.e1-.e13.
9. Taylor PD, Samuelsson AM, Poston L. Maternal obesity and the developmental programming of hypertension: a role for leptin. Acta Physiol (Oxf). 2014;210(3):508-23.
10. Godfrey KM, Reynolds RM, Prescott SL, Nyirenda M, Jaddoe VW, Eriksson JG, et al. Influence of maternal obesity on the long-term health of offspring. Lancet Diabetes Endocrinol. 2017;5(1):53-64.
11. Catalano PM. Obesity and pregnancy--the propagation of a viscous cycle? J Clin Endocrinol Metab. 2003;88(8):3505-6.
12. Aune D, Saugstad OD, Henriksen T, Tonstad S. Maternal body mass index and the risk of fetal death, stillbirth, and infant death: a systematic review and meta-analysis. Jama. 2014;311(15):1536-46.
13. Wang Y, Tang S, Xu S, Weng S, Liu Z. Maternal Body Mass Index and Risk of Autism Spectrum Disorders in Offspring: A Meta-analysis. Sci Rep. 2016;6:34248.
14. Forthun I, Wilcox AJ, Strandberg-Larsen K, Moster D, Nohr EA, Lie RT, et al. Maternal Prepregnancy BMI and Risk of Cerebral Palsy in Offspring. Pediatrics. 2016;138(4).
15. Sanchez CE, Barry C, Sabhlok A, Russell K, Majors A, Kollins SH, et al. Maternal pre-pregnancy obesity and child neurodevelopmental outcomes: a meta-analysis. Obes Rev. 2018;19(4):464-84.
16. Cochrane ALK, Murphy MP, Ozanne SE, Giussani DA. Pregnancy in obese women and mechanisms of increased cardiovascular risk in offspring. Eur Heart J. 2024;45(48):5127-45.
17. Hedermann G, Hedley PL, Thagaard IN, Krebs L, Ekelund CK, Sørensen TIA, et al. Maternal obesity and metabolic disorders associate with congenital heart defects in the offspring: A systematic review. PLoS One. 2021;16(5):e0252343.
18. Cai GJ, Sun XX, Zhang L, Hong Q. Association between maternal body mass index and congenital heart defects in offspring: a systematic review. Am J Obstet Gynecol. 2014;211(2):91-117.

19. Barker DJ. Fetal origins of coronary heart disease. Bmj. 1995;311(6998):171-4.

20. Reynolds RM, Allan KM, Raja EA, Bhattacharya S, McNeill G, Hannaford PC, et al. Maternal obesity during pregnancy and premature mortality from cardiovascular event in adult offspring: follow-up of 1 323 275 person years. BMJ : British Medical Journal. 2013;347:f4539.

21. Barker DJ, Osmond C, Golding J, Kuh D, Wadsworth ME. Growth in utero, blood pressure in childhood and adult life, and mortality from cardiovascular disease. Bmj. 1989;298(6673):564-7.

22. Li G, Xiao Y, Estrella JL, Ducsay CA, Gilbert RD, Zhang L. Effect of fetal hypoxia on heart susceptibility to ischemia and reperfusion injury in the adult rat. J Soc Gynecol Investig. 2003;10(5):265-74.

23. Alexander BT. Placental insufficiency leads to development of hypertension in growth-restricted offspring. Hypertension. 2003;41(3):457-62.

24. Veille JC, Hanson R, Sivakoff M, Hoen H, Ben-Ami M. Fetal cardiac size in normal, intrauterine growth retarded, and diabetic pregnancies. Am J Perinatol. 1993;10(4):275-9.

25. Russell NE, Foley M, Kinsley BT, Firth RG, Coffey M, McAuliffe FM. Effect of pregestational diabetes mellitus on fetal cardiac function and structure. Am J Obstet Gynecol. 2008;199(3):312.e1-7.

26. Persson M, Cnattingius S, Villamor E, Söderling J, Pasternak B, Stephansson O, et al. Risk of major congenital malformations in relation to maternal overweight and obesity severity: cohort study of 1.2 million singletons. Bmj. 2017;357:j2563.

27. Patey O, Carvalho JS, Thilaganathan B. Perinatal changes in fetal cardiac geometry and function in diabetic pregnancy at term. Ultrasound Obstet Gynecol. 2019;54(5):634-42.

28. Thornburg KL. The programming of cardiovascular disease. J Dev Orig Health Dis. 2015;6(5):366-76.

29. Alharithi YJ, Phillips EA, Wilson TD, Couvillion SP, Nicora CD, Darakjian P, et al. Metabolomic and transcriptomic remodeling of bone marrow myeloid cells in response to maternal obesity. Am J Physiol Endocrinol Metab. 2025;328(2):E254-e71.

30. Calco GN, Alharithi YJ, Williams KR, Jacoby DB, Fryer AD, Maloyan A, et al. Maternal high-fat diet increases airway sensory innervation and reflex bronchoconstriction in adult offspring. Am J Physiol Lung Cell Mol Physiol. 2023;325(1):L66-l73.

31. Phillips EA, Alharithi YJ, Kadam L, Coussens LM, Kumar S, Maloyan A. Metabolic abnormalities in the bone marrow cells of young offspring born to mothers with obesity. Int J Obes (Lond). 2024;48(11):1542-51.

32. Montaniel KRC, Bucher M, Phillips EA, Li C, Sullivan EL, Kievit P, et al. Dipeptidyl peptidase IV inhibition delays developmental programming of obesity and metabolic disease in male offspring of obese mothers. J Dev Orig Health Dis. 2022;13(6):727-40.

33. Gu H, Smith ZD, Bock C, Boyle P, Gnirke A, Meissner A. Preparation of reduced representation bisulfite sequencing libraries for genome-scale DNA methylation profiling. Nat Protoc. 2011;6(4):468-81.

34. Carbone L, Davis BA, Fei SS, White A, Nevonen KA, Takahashi D, et al. Synergistic Effects of Hyperandrogenemia and Obesogenic Western-style Diet on Transcription and DNA Methylation in Visceral Adipose Tissue of Nonhuman Primates. Sci Rep. 2019;9(1):19232.

35. Harris CJ, Davis BA, Zweig JA, Nevonen KA, Quinn JF, Carbone L, et al. Age-Associated DNA Methylation Patterns Are Shared Between the Hippocampus and Peripheral Blood Cells. Front Genet. 2020;11:111.

36. Krueger F, Andrews SR. Bismark: a flexible aligner and methylation caller for Bisulfite-Seq applications. Bioinformatics. 2011;27(11):1571-2.

37. Law CW, Chen Y, Shi W, Smyth GK. voom: precision weights unlock linear model analysis tools for RNA-seq read counts. Genome Biology. 2014;15(2):R29.

38. Pedersen BS, Schwartz DA, Yang IV, Kechris KJ. Comb-p: software for combining, analyzing, grouping and correcting spatially correlated P-values. Bioinformatics. 2012;28(22):2986-8.

39. Chen EY, Tan CM, Kou Y, Duan Q, Wang Z, Meirelles GV, et al. Enrichr: interactive and collaborative HTML5 gene list enrichment analysis tool. BMC Bioinformatics. 2013;14(1):128.

40. McLean CY, Bristor D, Hiller M, Clarke SL, Schaar BT, Lowe CB, et al. GREAT improves functional interpretation of cis-regulatory regions. Nat Biotechnol. 2010;28(5):495-501.

41. Heinz S, Benner C, Spann N, Bertolino E, Lin YC, Laslo P, et al. Simple combinations of lineage-determining transcription factors prime cis-regulatory elements required for macrophage and B cell identities. Mol Cell. 2010;38(4):576-89.

42. Ruffell B, Au A, Rugo HS, Esserman LJ, Hwang ES, Coussens LM. Leukocyte composition of human breast cancer. Proc Natl Acad Sci U S A. 2012;109(8):2796-801.

43. Smith ZD, Meissner A. DNA methylation: roles in mammalian development. Nat Rev Genet. 2013;14(3):204-20.

44. Wu H, Zhang Y. Reversing DNA methylation: mechanisms, genomics, and biological functions. Cell. 2014;156(1-2):45-68.

45. Zhong J, Agha G, Baccarelli AA. The Role of DNA Methylation in Cardiovascular Risk and Disease. Circulation Research. 2016;118(1):119-31.

46. Pepin ME, Drakos S, Ha CM, Tristani-Firouzi M, Selzman CH, Fang JC, et al. DNA methylation reprograms cardiac metabolic gene expression in end-stage human heart failure. Am J Physiol Heart Circ Physiol. 2019;317(4):H674-h84.

47. Okamura K, Hagiwara-Takeuchi Y, Li T, Vu TH, Hirai M, Hattori M, et al. Comparative genome analysis of the mouse imprinted gene impact and its nonimprinted human homolog IMPACT: toward the structural basis for species-specific imprinting. Genome Res. 2000;10(12):1878-89.

48. Mardjuki R, Wang S, Carozza J, Zirak B, Subramanyam V, Abhiraman G, et al. Identification of the extracellular membrane protein ENPP3 as a major cGAMP hydrolase and innate immune checkpoint. Cell Rep. 2024;43(5):114209.

49. Stowe TR, Wilkinson CJ, Iqbal A, Stearns T. The centriolar satellite proteins Cep72 and Cep290 interact and are required for recruitment of BBS proteins to the cilium. Mol Biol Cell. 2012;23(17):3322-35.

50. Veera S, Tang F, Mourad Y, Kim S, Liu T, Li H, et al. A transcriptional regulatory mechanism of genes in the tricarboxylic acid cycle in the heart. Journal of Biological Chemistry. 2024;300(9):107677.

51. Nie S, Bronner ME. Dual developmental role of transcriptional regulator Ets1 in Xenopus cardiac neural crest vs. heart mesoderm. Cardiovasc Res. 2015;106(1):67-75.

52. Lee D, Park C, Lee H, Lugus JJ, Kim SH, Arentson E, et al. ER71 acts downstream of BMP, Notch, and Wnt signaling in blood and vessel progenitor specification. Cell Stem Cell. 2008;2(5):497-507.

53. Lee S, Lee DH, Park B-W, Kim R, Hoang AD, Woo S-K, et al. In vivo transduction of ETV2 improves cardiac function and induces vascular regeneration following myocardial infarction. Experimental & Molecular Medicine. 2019;51(2):1-14.

54. Lee DH, Kim TM, Kim JK, Park C. ETV2/ER71 Transcription Factor as a Therapeutic Vehicle for Cardiovascular Disease. Theranostics. 2019;9(19):5694-705.

55. Nishida K, Otsu K. Inflammation and metabolic cardiomyopathy. Cardiovascular Research. 2017;113(4):389-98.

56. Alexanian M, Padmanabhan A, Nishino T, Travers JG, Ye L, Pelonero A, et al. Chromatin remodelling drives immune cell–fibroblast communication in heart failure. Nature. 2024;635(8038):434-43.

57. Suthahar N, Meijers WC, Silljé HHW, de Boer RA. From Inflammation to Fibrosis-Molecular and Cellular Mechanisms of Myocardial Tissue Remodelling and Perspectives on Differential Treatment Opportunities. Curr Heart Fail Rep. 2017;14(4):235-50.

58. Toemen L, Gishti O, van Osch-Gevers L, Steegers EA, Helbing WA, Felix JF, et al. Maternal obesity, gestational weight gain and childhood cardiac outcomes: role of childhood body mass index. Int J Obes (Lond). 2016;40(7):1070-8.

59. Gademan MG, van Eijsden M, Roseboom TJ, van der Post JA, Stronks K, Vrijkotte TG. Maternal prepregnancy body mass index and their children's blood pressure and resting cardiac autonomic balance at age 5 to 6 years. Hypertension. 2013;62(3):641-7.

60. Guzzardi MA, Liistro T, Gargani L, Ait Ali L, D'Angelo G, Rocchiccioli S, et al. Maternal Obesity and Cardiac Development in the Offspring: Study in Human Neonates and Minipigs. JACC Cardiovasc Imaging. 2018;11(12):1750-5.

61. Ekici Avci M, Tosun Ö. Evaluation of subclinical atherosclerosis and cardiac functions in children of mothers with gestational diabetes and maternal obesity. Cardiol Young. 2023;33(7):1157-64.

62. Ferey JLA, Boudoures AL, Reid M, Drury A, Scheaffer S, Modi Z, et al. A maternal high-fat, high-sucrose diet induces transgenerational cardiac mitochondrial dysfunction independently of maternal mitochondrial inheritance. Am J Physiol Heart Circ Physiol. 2019;316(5):H1202-h10.

63. Ahmed A, Liang M, Chi L, Zhou YQ, Sled JG, Wilson MD, et al. Maternal obesity persistently alters cardiac progenitor gene expression and programs adult-onset heart disease susceptibility. Mol Metab. 2021;43:101116.

64. Loche E, Blackmore HL, Carpenter AA, Beeson JH, Pinnock A, Ashmore TJ, et al. Maternal diet-induced obesity programmes cardiac dysfunction in male mice independently of post-weaning diet. Cardiovasc Res. 2018;114(10):1372-84.

65. Ingul CB, Lorås L, Tegnander E, Eik-Nes SH, Brantberg A. Maternal obesity affects fetal myocardial function as early as in the first trimester. Ultrasound Obstet Gynecol. 2016;47(4):433-42.

66. Vaughan OR, Rosario FJ, Chan J, Cox LA, Ferchaud-Roucher V, Zemski-Berry KA, et al. Maternal obesity causes fetal cardiac hypertrophy and alters adult offspring myocardial metabolism in mice. J Physiol. 2022;600(13):3169-91.

67. Nomura S, Satoh M, Fujita T, Higo T, Sumida T, Ko T, et al. Cardiomyocyte gene programs encoding morphological and functional signatures in cardiac hypertrophy and failure. Nature Communications. 2018;9(1):4435.

68. Siddeek B, Mauduit C, Chehade H, Blin G, Liand M, Chindamo M, et al. Long-term impact of maternal high-fat diet on offspring cardiac health: role of micro-RNA biogenesis. Cell Death Discovery. 2019;5(1):71.

69. Huang Y, Yan X, Zhao JX, Zhu MJ, McCormick RJ, Ford SP, et al. Maternal obesity induces fibrosis in fetal myocardium of sheep. Am J Physiol Endocrinol Metab. 2010;299(6):E968-75.

70. Nevers T, Salvador AM, Grodecki-Pena A, Knapp A, Velázquez F, Aronovitz M, et al. Left Ventricular T-Cell Recruitment Contributes to the Pathogenesis of Heart Failure. Circ Heart Fail. 2015;8(4):776-87.

71. Maloyan A, Muralimanoharan S, Huffman S, Cox LA, Nathanielsz PW, Myatt L, et al. Identification and comparative analyses of myocardial miRNAs involved in the fetal response to maternal obesity. Physiol Genomics. 2013;45(19):889-900.

72. Spitkovsky D, Sasse P, Kolossov E, Böttinger C, Fleischmann BK, Hescheler J, et al. Activity of complex III of the mitochondrial electron transport chain is essential for early heart muscle cell differentiation. The FASEB Journal. 2004;18(11):1300-2.

73. Wu C, Zhang Z, Zhang W, Liu X. Mitochondrial dysfunction and mitochondrial therapies in heart failure. Pharmacological Research. 2022;175:106038.

74. Bucher M, Montaniel KRC, Myatt L, Weintraub S, Tavori H, Maloyan A. Dyslipidemia, insulin resistance, and impairment of placental metabolism in the offspring of obese mothers. J Dev Orig Health Dis. 2021;12(5):738-47.

75. Mele J, Muralimanoharan S, Maloyan A, Myatt L. Impaired mitochondrial function in human placenta with increased maternal adiposity. Am J Physiol Endocrinol Metab. 2014;307(5):E419-25.

76. Wang J, Ma H, Tong C, Zhang H, Lawlis GB, Li Y, et al. Overnutrition and maternal obesity in sheep pregnancy alter the JNK-IRS-1 signaling cascades and cardiac function in the fetal heart. Faseb j. 2010;24(6):2066-76.

77. Preston CC, Larsen TD, Eclov JA, Louwagie EJ, Gandy TCT, Faustino RS, et al. Maternal High Fat Diet and Diabetes Disrupts Transcriptomic Pathways That Regulate Cardiac Metabolism and Cell Fate in Newborn Rat Hearts. Front Endocrinol (Lausanne). 2020;11:570846.

78. Fernández-Verdejo R, Gutiérrez-Pino J, Hayes-Ortiz T, Zbinden-Foncea H, Cabello-Verrugio C, Valero-Breton M, et al. Metabolic flexibility to lipid during exercise is not associated with metabolic health outcomes in individuals without obesity. Scientific Reports. 2024;14(1):28642.

79. van de Weijer T, Sparks LM, Phielix E, Meex RC, van Herpen NA, Hesselink MKC, et al. Relationships between Mitochondrial Function and Metabolic Flexibility in Type 2 Diabetes Mellitus. PLOS ONE. 2013;8(2):e51648.

80. Wilson RM, Messaoudi I. The impact of maternal obesity during pregnancy on offspring immunity. Mol Cell Endocrinol. 2015;418 Pt 2(0 2):134-42.

81. Levy O. Innate immunity of the human newborn: distinct cytokine responses to LPS and other Toll-like receptor agonists. J Endotoxin Res. 2005;11(2):113-6.

82. Ibrahim MH, Moustafa AN, Saedii AAF, Hassan EE. Cord blood erythropoietin and cord blood nucleated red blood cells for prediction of adverse neonatal outcome associated with maternal obesity in term pregnancy: prospective cohort study. J Matern Fetal Neonatal Med. 2017;30(18):2237-42.

83. Gonzalez-Espinosa LO, Montiel-Cervantes LA, Guerra-Márquez A, Peñaflor-Juárez K, Reyes-Maldonado E, Vela-Ojeda J. Maternal obesity associated with increase in natural killer T cells and CD8+ regulatory T cells in cord blood units. Transfusion. 2016;56(5):1075-81.

84. Yan X, Huang Y, Wang H, Du M, Hess BW, Ford SP, et al. Maternal obesity induces sustained inflammation in both fetal and offspring large intestine of sheep. Inflamm Bowel Dis. 2011;17(7):1513-22.

85. Wilson RM, Marshall NE, Jeske DR, Purnell JQ, Thornburg K, Messaoudi I. Maternal obesity alters immune cell frequencies and responses in umbilical cord blood samples. Pediatr Allergy Immunol. 2015;26(4):344-51.

86. Muralimanoharan S, Guo C, Myatt L, Maloyan A. Sexual dimorphism in miR-210 expression and mitochondrial dysfunction in the placenta with maternal obesity. Int J Obes (Lond). 2015;39(8):1274-81.

87. Phillips EA, Hendricks N, Bucher M, Maloyan A. Vitamin D Supplementation Improves Mitochondrial Function and Reduces Inflammation in Placentae of Obese Women. Front Endocrinol (Lausanne). 2022;13:893848.

88. Wong NR, Mohan J, Kopecky BJ, Guo S, Du L, Leid J, et al. Resident cardiac macrophages mediate adaptive myocardial remodeling. Immunity. 2021;54(9):2072-88.e7.

89. Mylonas KJ, Jenkins SJ, Castellan RF, Ruckerl D, McGregor K, Phythian-Adams AT, et al. The adult murine heart has a sparse, phagocytically active macrophage population that expands through monocyte recruitment and adopts an 'M2' phenotype in response to Th2 immunologic challenge. Immunobiology. 2015;220(7):924-33.

90. Rurik JG, Aghajanian H, Epstein JA. Immune Cells and Immunotherapy for Cardiac Injury and Repair. Circ Res. 2021;128(11):1766-79.

91. Tkacz K, Rolski F, Czepiel M, Działo E, Siedlar M, Eriksson U, et al. Haploinsufficient Rock1(+/-) and Rock2(+/-) Mice Are Not Protected from Cardiac Inflammation and Postinflammatory Fibrosis in Experimental Autoimmune Myocarditis. Cells. 2020;9(3).
92. Shi Y, Zhang H, Huang S, Yin L, Wang F, Luo P, et al. Epigenetic regulation in cardiovascular disease: mechanisms and advances in clinical trials. Signal Transduction and Targeted Therapy. 2022;7(1):200.
93. Reichetzeder C. Overweight and obesity in pregnancy: their impact on epigenetics. European Journal of Clinical Nutrition. 2021;75(12):1710-22.
94. Si J, Meir AY, Hong X, Wang G, Huang W, Pearson C, et al. Maternal pre-pregnancy BMI, offspring epigenome-wide DNA methylation, and childhood obesity: findings from the Boston Birth Cohort. BMC Medicine. 2023;21(1):317.
95. Marchlewicz EH, Dolinoy DC, Tang L, Milewski S, Jones TR, Goodrich JM, et al. Lipid metabolism is associated with developmental epigenetic programming. Sci Rep. 2016;6:34857.
96. Agarwal P, Morriseau TS, Kereliuk SM, Doucette CA, Wicklow BA, Dolinsky VW. Maternal obesity, diabetes during pregnancy and epigenetic mechanisms that influence the developmental origins of cardiometabolic disease in the offspring. Crit Rev Clin Lab Sci. 2018;55(2):71-101.
97. Yang QY, Liang JF, Rogers CJ, Zhao JX, Zhu MJ, Du M. Maternal obesity induces epigenetic modifications to facilitate Zfp423 expression and enhance adipogenic differentiation in fetal mice. Diabetes. 2013;62(11):3727-35.
98. Schlabritz-Loutsevitch N, Apostolakis-Kyrus K, Krutilina R, Hubbard G, Kocak M, Janjetovic Z, et al. Pregnancy-driven cardiovascular maternal miR-29 plasticity in obesity. J Med Primatol. 2016;45(6):297-303.
99. Martin SS, Aday AW, Allen NB, Almarzooq ZI, Anderson CAM, Arora P, et al. 2025 Heart Disease and Stroke Statistics: A Report of US and Global Data From the American Heart Association. Circulation.0(0).

FIGURE LEGENDS

Figure 1. **Birthweight- and age-dependent body weight changes in Off-RD and Off-HFD**. A, Mouse model of maternal diet-induced obesity. B, Birthweights of Off-RD and Off-HFD mice. C,D, Change in body weights from weaning to six months of age in male (C) and female (D) Off-RD and Off-HFD mice. Data were analyzed by two-way ANOVA followed by multiple unpaired *t*-tests. N= 20–44/group of maternal diet/age. Data are represented as either individual values (B) or as mean±SEM (C-D). *P* values are either shown (B) or labeled with * when $p<0.05$ for Off-HFD vs. Off-RD at each age (C-D).

Figure 2. **Maternal high-fat diet feeding changes metabolic phenotype in offspring.** A-G, Oxygen consumption and respiratory exchange ratio (RER) in four-month-old male and female Off-RD and Off-HFD mice. A-B, Oxygen consumption curves calculated for male (A) and female (B) mice over a 24-hour period (12 hours active and 12 hours rest). C-D, RER in male (C) and female (D) Off-RD and Off-HFD mice over active and rest periods. E-F, Shift in RER between active and rest periods in Off-RD (E) and Off-HFD (F) mice. Male and female data are pooled. *, $p<0.05$ calculated by multiple unpaired *t*-tests with false discovery rate (FDR) <0.01. G, Average 24-hour RER in Off-RD and Off-HFD, male and female data pooled. Data are represented as individual values with lines at mean with SEM; *p*-values are shown, calculated by t-test. N=5-8/group of maternal diet/sex.

Figure 3. Cardio-metabolic changes in the offspring of HFD-fed mothers. A-B, Heart weight-to-body weight ratio in newly weaned (A) and six-month-old (B) Off-RD and Off-HFD mice fed a normal chow diet. N=38-62 mice/group of maternal diet. C, Liver weight-to-body weight ratio, n=10/experimental group. D, Tail cuff-measured mean arterial pressure in male and female Off-RD and Off-HFD mice, n=5-7 mice/sex/group of maternal diet. E-H, Changes in blood lipids in Off-HFD vs. Off-RD, including total cholesterol (E), triglycerides (F), phospholipids (G), and non-esterified fatty acids (NEFA, H). Data were analyzed by multiple *t*-tests with FDR<0.01. Data are represented as individual values with lines at mean with SEM. N=5/sex/group of maternal diet, 20 animals overall. Data from males and females were pooled. *P*-values are shown.

Figure 4. Echocardiographic evaluation of adult male and female Off-RD and Off-HFD mice. A, Representative parasternal long-axis B-mode images of the left ventricle and short axis. B-F, Sex-dependent changes in diastolic (B) and systolic (C) intra-ventricular septum thickness; and diastolic (D) and systolic (E) left ventricular posterior wall thickness. F, Quantification of left ventricular ejection fraction (EF) expressed in percent (%). N=5-

9/sex/group of maternal diet. Data are represented as individual values for males (left) and females (right) with lines at mean with SEM. Significant differences was determined by Mann-Whitney test followed by unpaired *t*□test; p-values are shown.

Figure 5. **Mapping and comparisons of the DNA methylomes of newly weaned Off-RD and OFF-HFD.** A, Heatmap and unsupervised hierarchical clustering of the 12 Off-RD and Off-HFD samples based on individual DNA methylation status. B, Bar graphs showing canonical pathways identified by Ingenuity Pathway Analysis as enriched among differentially methylated genes. C, Volcano plot showing statistical significance (-log(*p*-value)) vs. change in methylation percentage. Several differentially methylated genes with highest amplitudes of change are labeled. Grey line indicates the threshold for significance (-log(0.05)=1.3). Data from males and females were pooled.

Figure 6. **Histopathological evaluations.** A, H&E staining of representative heart sections from Off-RD and Off-HFD mice showing mild perivascular inflammation in Off-HFD mice. Scale bar 60 µm. B, Masson's trichrome staining of cardiac sections. Scale bars 100 µm (Off-RD), and 100 and 80 µm (Off-HFD). C, Quantification of cardiomyocyte cross-sectional area from trichrome-stained images. Overall, 135-150 cardiomyocytes were analyzed in each group of maternal diet. D, Quantification of fibrosis. Blue-stained areas in trichrome staining were color-thresholded using NIH ImageJ and quantitated. Data from males and females were pooled. Data are represented as individual values with lines at mean with SEM. N=3/sex/group of maternal diet, *p*-values are shown.

F**igure 7. Ultrastructural and metabolic changes in the heart of Off-HFD mice.** A, Transmission electron microscopy from 16-week-old mice showing dysregulations in mitochondrial alignment and increased accumulation of autolysosomes (asterisks) and lipid droplets (yellow arrows) in Off-HFD vs. Off-RD. Inserts present magnified views of autophagic vacuoles and lipid droplets. Scale bar: 1 mm. B-H, Western blots for expression of subunits of the mitochondrial electron transport chain, with Vinculin as loading control. B, Cartoon of the mitochondrial complexes, created with Biorender.com. C, Representative western blots for male and female Off-RD and Off-HFD. D-H, Quantification data for complex 1 (D), 2 (E), 3 (F), 4 (G), and 5 (H). Data were analyzed with two-way ANOVA followed by *t*-test. Data are represented as individual values with lines at mean with SEM. *P*-values are shown. Data from males and females were pooled. N=8/group of maternal diet.

Figure 8. **Flow cytometric analysis of immune cell populations in the heart of 16-week-old Off-RD and Off-HFD mice.** Changes in heart immune complexity in Off-HFD as compared with Off-RD mice include: a decrease in CD45+ cells (A); increases in CD11b/F480 macrophages (B) and CD11b-/F480+ resident macrophages (C); and decrease in the percentage of CD3+ cells (D), including both CD4+ (E) and CD8+ T-cells (F). Data are represented as individual values with lines at mean with SEM. N=9-12/group of maternal diet, *p*-values are shown.

A
6 weeks
♀
Breeding
8 weeks pre-pregnancy
Pregnancy
Weaning
Maternal Regular or High Fat Diet
(RD or HFD)
Young
Off-RD
Off-HFD
Adult
Off-RD
Off-HFD
Regular Diet
B
<0.0001
Birthweight (grams)
2.0
1.5
1.0
0.5
Off-RD
Off-HFD
C
Males
Off-RD
Off-HFD
Body weight (grams)
50
40
30
20
10
*
*
*
*
0
2
4
6
Age (months)
D
Females
Off-RD
Off-HFD
Body weight (grams)
40
30
20
10
0
*
*
*
*
0
2
4
6
Age (months)

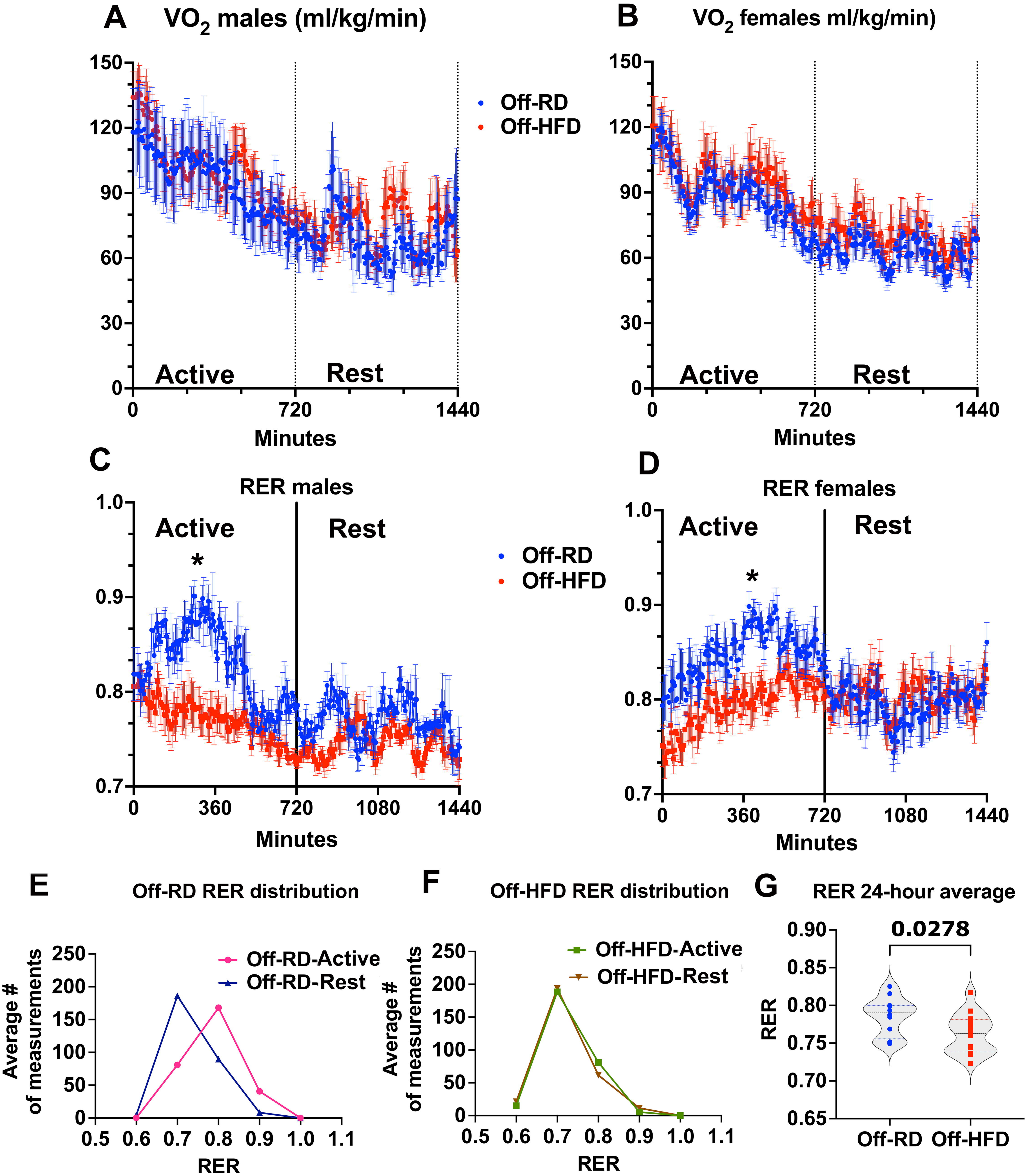
A
VO2 males (ml/kg/min)
B
VO2 females ml/kg/min)
Off-RD
Off-HFD
Active
Rest
Minutes
0
720
1440
150
120
90
60
30
0
C
RER males
D
RER females
Active
Rest
*
Off-RD
Off-HFD
1.0
0.9
0.8
0.7
0
360
720
1080
1440
Minutes
E
Off-RD RER distribution
Off-RD-Active
Off-RD-Rest
Average # of measurements
250
200
150
100
50
0
0.5
0.6
0.7
0.8
0.9
1.0
1.1
RER
F
Off-HFD RER distribution
Off-HFD-Active
Off-HFD-Rest
Average # of measurements
RER
G
RER 24-hour average
0.0278
RER
0.90
0.85
0.80
0.75
0.70
0.65
Off-RD
Off-HFD

A
Heart Weight/Body Weigh
0.0005
1×10-2
8×10-3
6×10-3
4×10-3
2×10-3
0
Young
Off-RD
Off-HFD
B
Heart Weight/Body Weight
<0.0001
1.6×10-2
1.2×10-2
8.0×10-3
4.0×10-3
0.0
Adult
Off-RD
Off-HFD
C
Liver Weight/Body Weight
0.4617
8
6
4
2
0
Off-RD
Off-HFD
D
Off-RD
Off-HFD
Mean Arterial Pressure (mmHg)
<0.05
ns
180
160
140
120
100
Males
Females
E
Total Cholesterol (mg/dL)
Blood Lipids
0.0371
200
150
100
50
0
Off-RD
Off-HFD
F
Triglycerides (mg/dL)
0.0082
250
200
150
100
50
0
Off-RD
Off-HFD
G
Phospholipids (mg/dL)
<0.0001
150
100
50
0
Off-RD
Off-HFD
H
NEFA (mEq/L)
0.0015
5
4
3
2
1
0
Off-RD
Off-HFD

A
PSLAX
SAX
Off-RD
Off-HFD
Male Off-RD
Male Off-HFD
Female Off-RD
Female Off-HFD
B
IVS;d
0.0140
1.0
0.8
0.6
0.4
0.2
0.0
Off-RD
Off-HFD
Off-RD
Off-HFD
C
IVS:s
1.5
1.0
0.5
0.0
Off-RD
Off-HFD
Off-RD
Off-HFD
D
LVPW,d
1.5
1.0
0.5
0.0
Off-RD
Off-HFD
Off-RD
Off-HFD
E
LVPW,s
0.0280
1.5
1.0
0.5
0.0
Off-RD
Off-HFD
Off-RD
Off-HFD
F
EF (%)
0.0005
0.0081
80
60
40
20
0
Off-RD
Off-HFD
Off-RD
Off-HFD

A
row min
row max
id
F1- Off-RD
F2-Off-RD
F3-Off-RD
F4-Off-RD
M1-Off-RD
M2-Off-RD
F2-Off-HFD
F3-Off-HFD
F4-Off-HFD
M2-Off-HFD
M3-Off-HFD
M4-Off-HFD
id
Commd1
Arhgap22
Ip6k3
Mcf2l
Psd3
Eng
Cmip
Prex1
Impact
Clmp
Pecam1
Elk3
Epas1
Npc1
Rps6ka2
Dock9
Rhobtb1
Sh3pxd2a
Grip2
Asap2
Xkr4
Ppcdc
Trappc9
Arhgef10l
Syf2
Cops4
Mcm8
Khdrbs2
Prkra
Srxn1
Mdga1
Zfx
B
Threshold
Cell Death and Survival
Cell Morphology
Cellular Compromise
Cell Morphology
Cardiovascular System Development
Cardiovascular Disease
Cellular Growth and Proliferation
Cellular Function and Maintenance
Cellular Assembly and Organization
Immunological Disease
Cancer
Cellular Development
Cell Cycle
Inflammatory Response
Cell Signaling and Interaction
0.0
1.3
2.6
3.9
-Log(p-value)
C
20
18
16
14
12
10
8
6
4
2
0
-Log(p-value)
Impact
Pecam1
Lamtor3
Nfkbil1
Atp6v1g1
Cebpa
Twf1
Notch1
-60
-40
-20
0
20
40
Change in methylation percentage

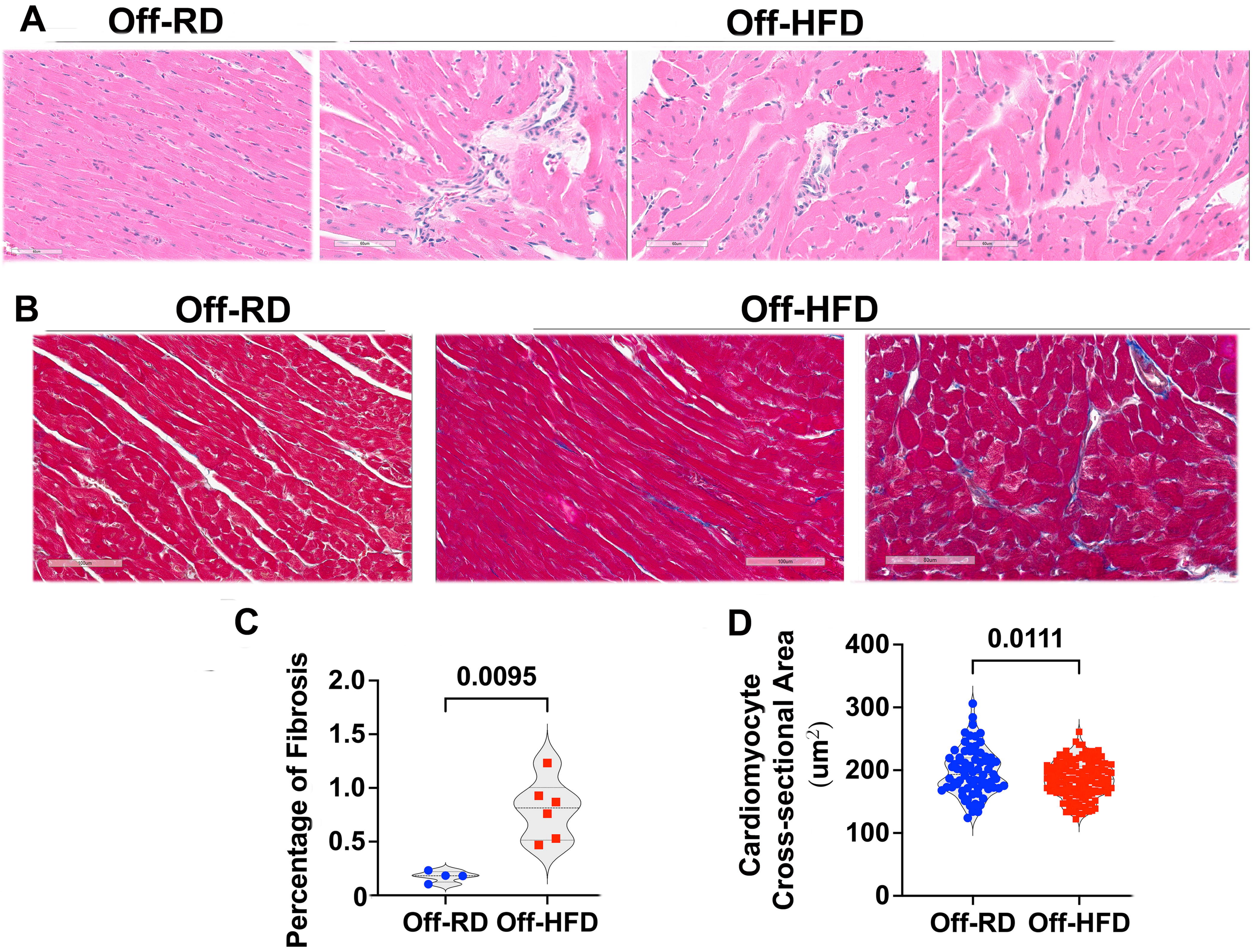
A
Off-RD
Off-HFD
60um
60um
60um
60um
B
Off-RD
Off-HFD
100um
100um
80um
C
Percentage of Fibrosis
2.0
1.5
1.0
0.5
0
0.0095
Off-RD
Off-HFD
D
Cardiomyocyte Cross-sectional Area (um^2)
400
300
200
100
0
0.0111
Off-RD
Off-HFD

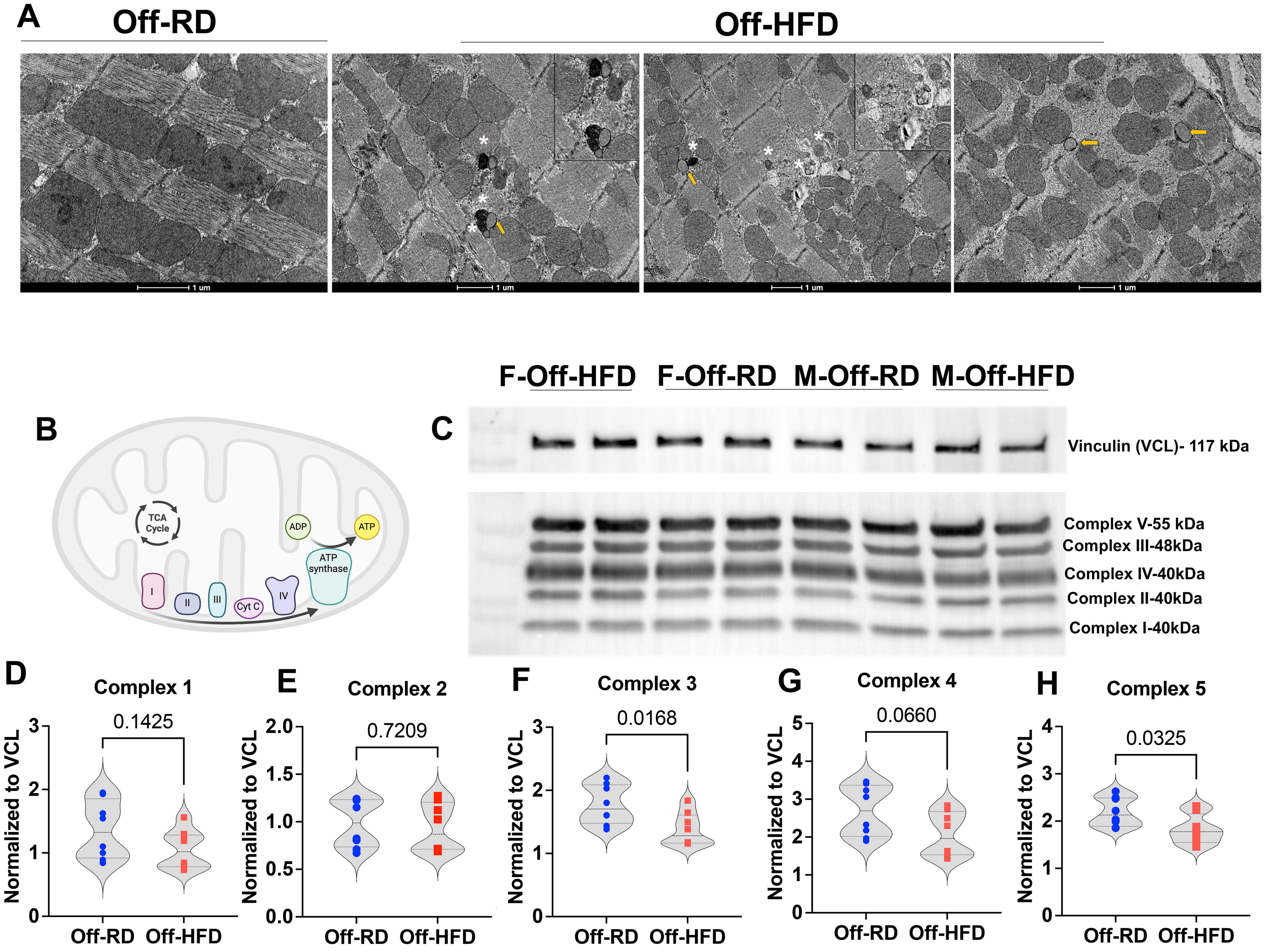
A
Off-RD
Off-HFD
1 um
1 um
1 um
1 um
B
TCA Cycle
ADP
ATP
ATP synthase
I
II
III
Cyt C
IV
C
F-Off-HFD
F-Off-RD
M-Off-RD
M-Off-HFD
Vinculin (VCL)- 117 kDa
Complex V-55 kDa
Complex III-48kDa
Complex IV-40kDa
Complex II-40kDa
Complex I-40kDa
D
Complex 1
0.1425
Normalized to VCL
0
1
2
3
Off-RD
Off-HFD
E
Complex 2
0.7209
Normalized to VCL
0.0
0.5
1.0
1.5
2.0
Off-RD
Off-HFD
F
Complex 3
0.0168
Normalized to VCL
0
1
2
3
Off-RD
Off-HFD
G
Complex 4
0.0660
Normalized to VCL
0
1
2
3
4
5
Off-RD
Off-HFD
H
Complex 5
0.0325
Normalized to VCL
0
1
2
3
4
Off-RD
Off-HFD

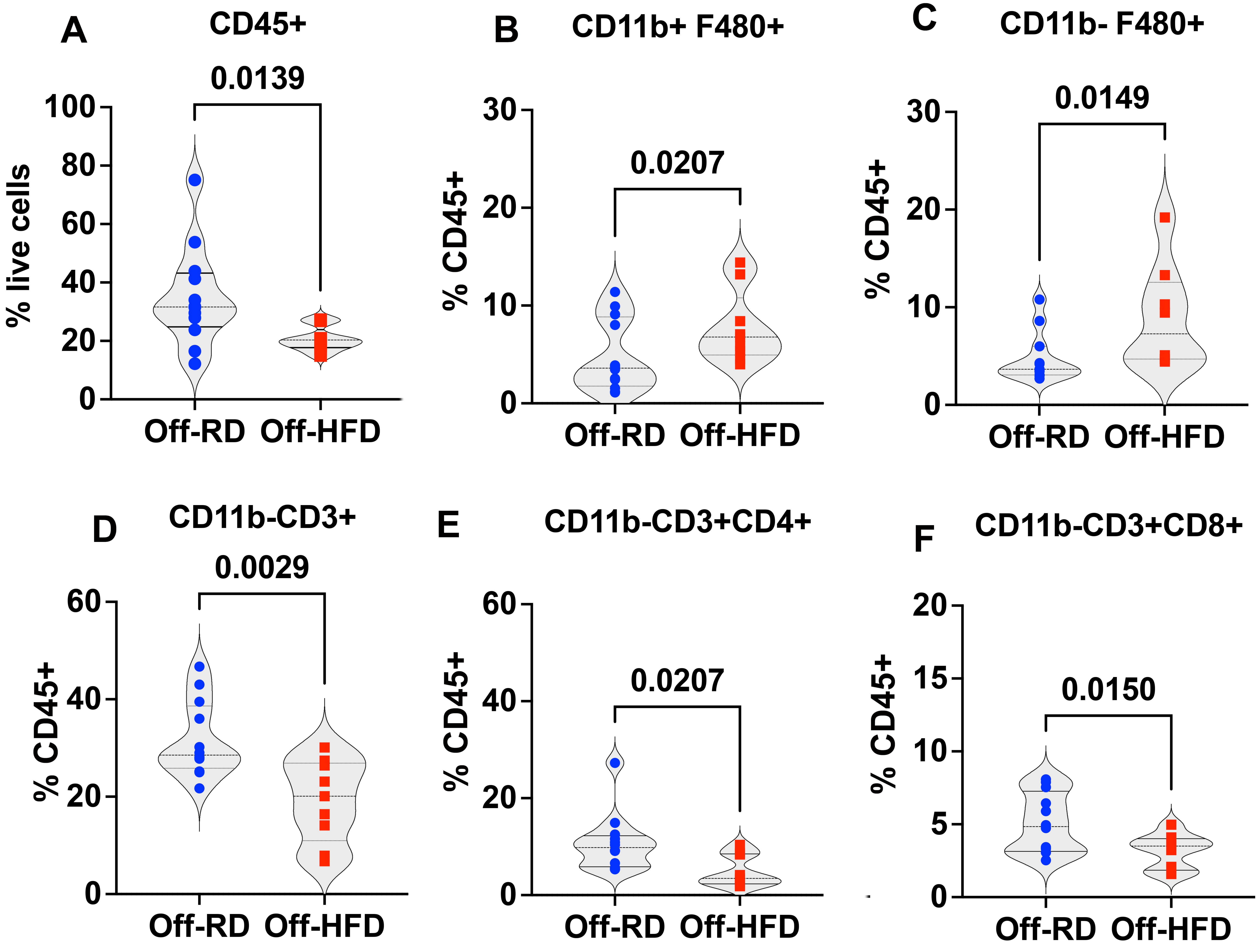
A
CD45+
0.0139
% live cells
100
80
60
40
20
0
Off-RD
Off-HFD
B
CD11b+ F480+
0.0207
% CD45+
30
20
10
0
Off-RD
Off-HFD
C
CD11b- F480+
0.0149
% CD45+
30
20
10
0
Off-RD
Off-HFD
D
CD11b-CD3+
0.0029
% CD45+
60
40
20
0
Off-RD
Off-HFD
E
CD11b-CD3+CD4+
0.0207
% CD45+
60
40
20
0
Off-RD
Off-HFD
F
CD11b-CD3+CD8+
0.0150
% CD45+
20
15
10
5
0
Off-RD
Off-HFD